Four dimensional visualization of highly transient fuel sprays by microsecond quantitative x-ray tomography

Xin Liu,[1,a)] Kyoung-Su Im,[1] Yujie Wang,[1] Jin Wang,[1,b)] Mark W. Tate,[2] Alper Ercan,[2] Daniel R. Schuette,[2] and Sol M. Gruner[2]
[1]*Advanced Photon Source, Argonne National Laboratory, Argonne, Illinois 60439, USA*
[2]*Cornell University, Ithaca, New York 14853, USA*

(Received 4 September 2008; accepted 19 November 2008; published online 23 February 2009)

An ultrafast x-ray microtomography technique based on synchrotron x rays and a fast-framing x-ray detector was developed to reconstruct the highly transient sprays in four dimensions with microsecond-temporal resolution in the near-nozzle region. The time-resolved quantitative fuel distribution allowed a realistic numerical fluid dynamic simulation with initial conditions based on the measurement, which demonstrates that the fuel has completed the primary breakup upon exiting the nozzle. The secondary-breakup-based simulation agrees well with the experimental fuel-volume fraction distribution, which challenges most existing simulation assumptions and results. © *2009 American Institute of Physics*. [DOI: 10.1063/1.3048563]

High-pressure high-speed sprays have vast industrial and consumer applications. Specifically, liquid-fuel sprays are part of energy sources for propulsion and transportation systems including internal combustion engines. Realistic fuel spray characterization, such as atomization and mixing with air in a cylinder, is crucial for a realistic combustion simulation.[1,2] Despite their longstanding multitude of uses, the fundamental physics that governs the spray flow formation in high-speed jets is not well understood. The most developed theory so far to explain the atomization process is that the surface instability waves lead to disintegration of the liquid jet into droplets characterized as primary breakup.[3] This theory can explain the breakup of laminar jets injected at low pressure and from a nozzle with relatively simple geometry (i.e., a round liquid jet).[4] However, understanding the breakups of liquid jets in regimes beyond the capillary-wave-controlled (low-velocity) cases has not been possible.[3–5] Traditional visualization techniques have not provided detailed information about the morphology of high-pressure sprays close to the nozzle, including the liquid breakup mechanism or the spray mass distribution.[6–8] Here, we report the development of ultrafast (microsecond) synchrotron x-ray-based tomography to interrogate the fundamental breakup phenomenon associated with the hollow-cone gasoline spray in the near-nozzle region. The total duration of the high-speed spray is only about 1 ms. The ultrafast temporal resolution was achieved by intense synchrotron x rays and an ultrafast detector.[9,10]

The experiment was performed at the D-1 beamline of the Cornell High Energy Synchrotron Source (CHESS) with preliminary experiments done at the 1-BM beamline at the Advanced Photon Source (APS). The experiment setup is described in EPAPS document #1[11] in detail. Briefly, at CHESS, x-rays produced by synchrotron radiation are monochromatized to 6.0 keV (energy bandwidth about 1%) using a double-multilayer monochromator. This x-ray energy is optimal for probing the fuel, a blend of a calibration fluid and a cerium-containing fuel additive.

The tomography spray chamber can be motorized to rotate and to translate in precise steps while the x-ray source and the detector are stationary, so that the sprays can be imaged from different orientations. The liquid fuel is injected into a quiescent gas atmosphere by an outward-opening annular slit-type nozzle to form a high-speed hollow-cone spray. The injection pressure is 7 MPa and the nominal injection duration of the spray is 1 ms.[11]

Downstream from the spray chamber is the microsecond, direct exposure x-ray camera, a pixel array detector (PAD), which was developed at Cornell University. The pixel pitch of the PAD is 150×150 μm^2. The exposure time per frame is set to 5.13 μs (twice the CHESS synchrotron period) with an interval between frames of 15.38 μs. Each frame is obtained by averaging 20 exposures of phase-locked individual injection events (operated at 1.15 Hz) to improve the signal-to-noise ratio. The parallel x-ray beam (perpendicular to the rotation axis) images the spray at a projection angle θ. After completion of the scans in temporal steps, the injection nozzle rotates a small angle $\Delta\theta(=1°)$ and the temporal scan is repeated. This process is continued until completion of 180° to collect a complete set of 180 projections. The full tomographic data set is obtained from multiple (>100 000) sprays to collect both spatial and temporal distributions of the spray in the near-nozzle region.[11]

Figure 1 shows the time-resolved projected density distribution of the fuel spray derived from the radiographic images at different projection angles.[11] Unprecedented details of the sprays can be readily observed from the high-quality images, such as global spray cone formation and its dynamics, local asymmetry, and streaks. More importantly, quantitative information, such as the mass distribution and mass flow rate, can be derived from these images from the attenuation law, as the two-dimensional (2D) fuel mass density (with a unit of *mass/unit-projection-area*) can be obtained by $M=(1/\mu_M)\ln(I_o/I)$, where I_o and I are the incident and detected x-ray intensities, respectively; μ_M is the mass attenuation coefficient of the fuel, which can be calibrated accurately.[11]

[a)]Present address: Mayo Clinic, Rochester, MN 55905. Electronic mail: liu.xin@mayo.edu.
[b)]Electronic mail: wangj@aps.anl.gov.

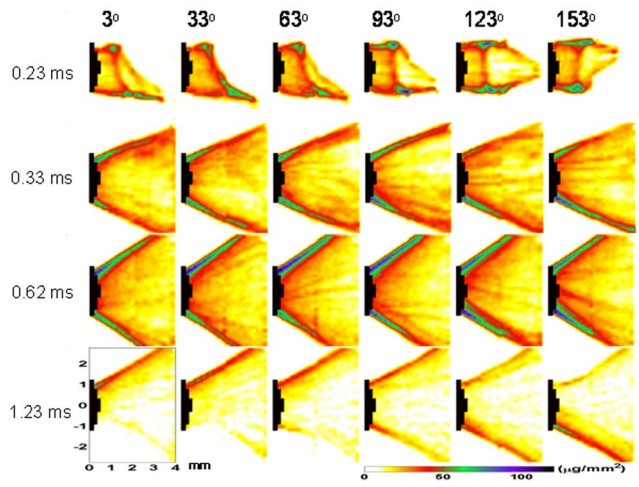

FIG. 1. (Color online) Examples of line-of-sight projected fuel mass density distribution derived from the radiographic images of the hollow-cone fuel sprays collected at 3°, 33°, 63°, 93°, 123°, and 153° projection angles at time instances of 0.23, 0.33, 0.62, and 1.23 ms after the SOI. The exposure time of each radiographic image is 5.13 μs. The rotation angular increment is 1°.

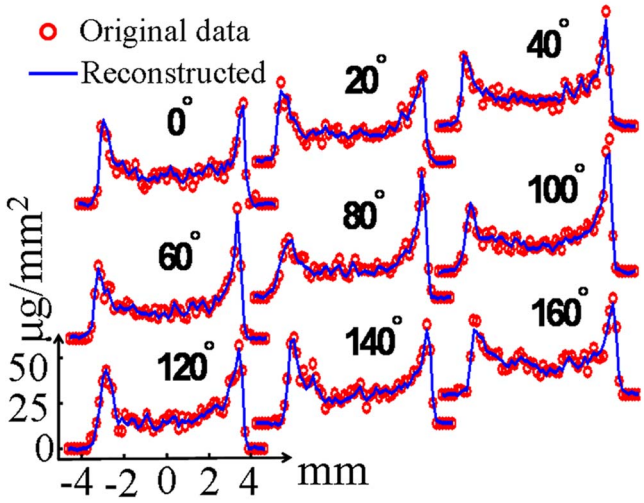

FIG. 3. (Color online) Comparison between the sinogram data from the measured radiographic images and the reconstructed spray distribution projected to different directions at 3.5 mm from the nozzle and 891 μs after the SOI.

The time-resolved density distribution can be reconstructed in three dimensions (3D) by the computed tomography technique,[12,13] assuming that the linear attenuation coefficient distribution of the spray cross section, $\mu_L(x,y)$, can be reconstructed from its line integrals. The fuel density distribution, $\rho(x,y)$, is derived based on $\rho(x,y)=\mu_L(x,y)/\mu_M$. The 3D fuel density distribution is, then, built upon all the reconstructed cross sections from the nozzle exit with a spatial resolution of 150 μm determined by the detector pixel size (see EPAPS document #2[11]).

Figure 2 shows the reconstructed 3D hollow-cone sprays at different time instances: the initial spray, the intermediate and steady sprays, and the sprays after the nozzle closed. An animation of the time-resolved fuel distribution is shown in EPAPS #3.[11] Although the sprays come out of a symmetrical nozzle orifice, the spray is highly asymmetric. The axially asymmetry can be caused by slight radial movement of the pintle and manufacture imperfections of the nozzle orifices.

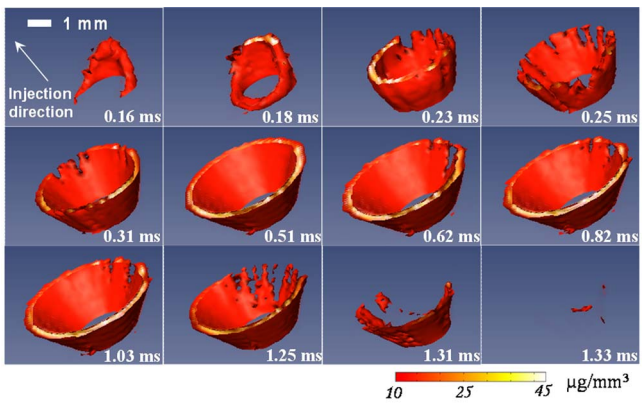

FIG. 2. (Color online) Reconstructed hollow-cone sprays based on 180 projections at each time instance from 0.16 (immediately after the start of injection) to 1.33 ms (end of injection) showing the development of the hollow-cone sprays throughout the 1.33 ms injection event. Detailed features of the spray including asymmetric fuel distributions can be readily observed. The time-resolved three-dimensional fuel distribution is reconstructed quantitatively as the false color represents the density of the fuel in unit of $\mu g/mm^3$.

We also observed that the cone angle varies during the whole injection process. The relatively steady state with fully opened cone angle only occurs about 25% of the duration. To visualize the highly asymmetric and transient nature of the spray, tomographic reconstruction has obvious advantages over the model-dependent method based on radiographic images,[14] which only yielded limited information about the fuel distribution.

The reconstructed spray is obtained by imaging sprays from many injection events in a phase-locked manner, which exerts a rigorous requirement on the spray repeatability. The validity and fidelity of the reconstruction can be verified by comparing the sinogram measured experimentally with the numerical projection of the reconstructed spray cross sections. Figure 3 shows the comparison at several view angles at 3.5 mm from the nozzle and 891 μs after the start of the injection (SOI). A good agreement between the two data sets is clearly demonstrated, which verified the repeatability of the spray and the reliability of the reconstruction.

We also discovered that the liquid volume fraction (VF) at the nozzle exit (<0.4) is substantially below the bulk liquid-fuel density (857.7 $\mu g/mm^3$, corresponding to VF $=1$), indicating that the liquid-jet primary breakup already happened inside the nozzle and well before reaching the nozzle exit. The exact mechanism leading to the liquid-jet breakup at the nozzle exit has yet to be understood. Most likely, the strong internal cavitation and turbulence caused by nozzle geometry and configuration[15–17] initiated the breakup.

To better understand how the spray behavior in this near-nozzle region affects the downstream spray morphology, we performed a computational fluid dynamics (CFD) simulation to understand the secondary breakup process. Obviously, simulating all the features observed experimentally would be extremely difficult and unrealistic due to the highly asymmetric and transient nature of the spray. Here, we choose a steady portion of the spray and focus on the azimuthally averaged (or axially symmetrized) density of the spray. We employed the stochastic particle injection method to model the discrete liquid parcels at the nozzle exit. By coupling the mass, the momentum, and the energy exchange between the

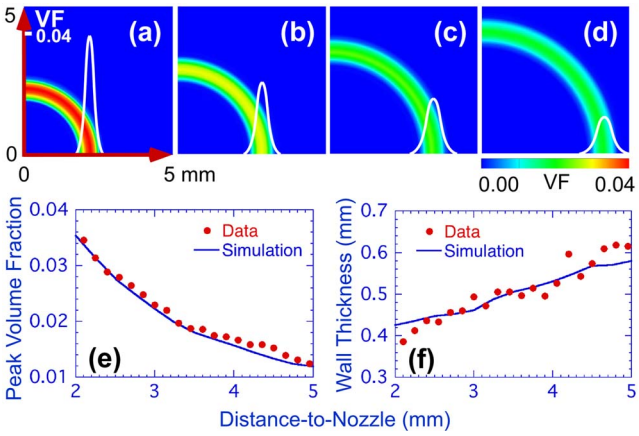

FIG. 4. (Color online) Comparison of liquid-fuel VF distribution between the CFD numerical simulation and experimental results. The simulated cross-sectional VF at selected spray cross sections (2, 3, 4, and 5 mm from the nozzle exit) are shown in (a), (b), (c), and (d), respectively. The radial distributions of the fuel VF at the selected cross-sectional planes are shown inside of (a), (b), (c), and (d), respectively. The measured and simulated peak fuel VF values in each cross-sectional planes are plotted in (e) and the hollow-cone spray wall thickness (full width at half maximum) in (f) along the spray axis.

droplets and gas phase during the secondary breakup process, we can mathematically describe the axial symmetric liquid/gas mixture emerging from the nozzle using a Taylor analogy breakup model.[18–20] By using the space-time conservation element and solution element method[21] and applying a conservation law to the individual liquid parcels, the fluid dynamics equations are directly solved in the Eulerian coordinate system. For computational efficiency, each computational parcel represents a number of child particles having the identical mechanical and thermodynamic properties.[22]

The simulation results of the cross-sectional VF at selected spray cross sections (2, 3, 4, and 5 mm from the nozzle exit) are plotted in Figs. 4(a)–4(d) in the first quadrant, respectively. To obtain a more quantitative comparison between the simulation and the data, the radial distributions of the fuel-volume fraction at the cross-sectional planes are overlaid in Figs. 4(a)–4(d), respectively. The CFD results have succeeded in capturing the experimental liquid-fuel-volume fraction distribution in the direction parallel to the spray axis [Fig. 4(e)] and the hollow-cone spray sheet (or wall) thickness (full width at half maximum) [Fig. 4(f)]. The agreement between the data and the simulation results is remarkably good.

Both experimental and numerical results show that the peak liquid-fuel VF values at each cross section (perpendicular to the spray axis) are well below unity even immediately at the orifice exit. In the CFD simulation, a hypothetic initial condition assuming a solid liquid sheet through the orifice would yield a much higher liquid VF in the near-nozzle region than that was measured experimentally. Therefore, we conclude that the secondary breakup is responsible for the atomization of the fuel outside of the nozzle. Both the experimental data and the simulation results show the absence of the primary breakup where the VF drops abruptly at the breakup length.[23]

To summarize, we have developed an ultrafast x-ray tomography and its utility of directly measuring the near-nozzle hollow-cone sprays in a highly quantitative and time-resolved manner. The tomography reconstructed fuel distribution and the simulation of the breakup model provide unique and realistic information to the fundamental understanding of the high-speed sprays. We also think that this technique is a sensitive probe and diagnostic tool for investigating other highly transient phenomena.

The work is supported by the U.S. Department of Energy under Contract No. DE-AC02-06CH11357 through an Argonne National Laboratory (ANL) LDRD grant. The authors would like to thank D. Shu, J. Liu, X. Li, C. F. Powell, and S. Cheong of ANL for their contributions. The authors would also like to thank the staff at APS 1-BM beamline and A. Woll, D. Smilgies and the staff at CHESS for their help with data collection. CHESS is funded by the U.S. National Science Foundation (NSF) and the U.S. National Institute of General Medical Sciences via NSF under Award No. DMR-9713424. PAD development was funded by DOE Grant Nos. DE-FG-0297ER14805 and DE-FG-0297ER62443.

[1] D. R. Cohn and J. B. Heywood, Phys. Today **55**(11), 12 (2002).
[2] F. Zhao, M.-C. Lai, and D. L. Harrington, Prog. Energy Combust. Sci. **25**, 437 (1999).
[3] R. D. Reitz and F. V. Bracco, Phys. Fluids **25**, 1730 (1982).
[4] P. Marmottant and E. Villermaux, J. Fluid Mech. **498**, 73 (2004).
[5] M. J. McCarthy and N. A. Molloy, Chem. Eng. J. **7**, 1 (1974).
[6] R. J. Adrian, Annu. Rev. Fluid Mech. **23**, 261 (1991).
[7] M. A. Coil, and P. V. Farrell, SAE Paper No. 950458, 1995.
[8] V. Sick and B. Stojkovic, Appl. Opt. **40**, 2435 (2001).
[9] S. L. Barna, J. A. Shepherd, M. W. Tate, R. L. Wixted, E. F. Eikenberry, and S. M. Gruner, IEEE Trans. Nucl. Sci. **44**, 950 (1997).
[10] G. Rossi, M. Renzi, E. F. Eikenberry, M. W. Tate, D. Bilderback, E. Fontes, R. Wixted, S. Barna, and S. M. Gruner, J. Synchrotron Radiat. **6**, 1096 (1999).
[11] See EPAPS Document No. E-APPLAB-93-069850 for a detailed description of experimental setup (#1), cross section view of fuel spray tomography reconstruction (#2) and four-dimensional movie of the reconstructed hollow-cone spray (#3). For more information on EPAPS, see http://www.aip.org/pubservs/epaps.html.
[12] A. C. Kak and M. Slaney, *Principles of Computed Tomographic Imaging* (IEEE, New York, 1999).
[13] X. Liu, J. Liu, X. Li, S. Cheong, D. Shu, J. Wang, M. W. Tate, A. Ercan, D. R. Schuette, M. J. Renzi, A. Woll, and S. M. Gruner, Proc. SPIE **5535**, 21 (2004).
[14] W. Cai, C. F. Powell, Y. Yue, S. Narayanan, J. Wang, M. W. Tate, M. J. Renzi, A. Ercan, E. Fontes, and S. M. Gruner, Appl. Phys. Lett. **83**, 1671 (2003).
[15] M. Kato, H. Kano, K. Date, T. Oya, K. Niizuma, SAE Paper No. 970052, 1997.
[16] H. Hiroyasu, Atomization Sprays **10**, 511 (2000).
[17] C. Ganippa, G. Bark, S. Andersson, and J. Chomiak, Exp. Fluids **36**, 627 (2004).
[18] Z. Han, S. Parrish, P. V. Farrell, and R. D. Reitz, Atomization Sprays **7**, 663 (1997).
[19] P. J. O'Rourke and A. A. Amsden, SAE Paper No. 872089, 1987.
[20] G. I. Taylor, *The Scientific Papers of Sir Geoffrey Ingram Taylor*, edited by G. K. Batchelor (Cambridge University Press, Cambridge, 1963), Vol. III.
[21] Z.-C. Zhang, S.-T. J. Yu, and S.-C. Chang, J. Comput. Phys. **175**, 168 (2002).
[22] J. K. Dukowicz, J. Comput. Phys. **35**, 229 (1980).
[23] Y. J. Wang, K. S. Im, K. F. Fezzaa, W. K. Lee, J. Wang, P. Micheli, and C. Laub, Appl. Phys. Lett. **89**, 151913 (2006).